Differential Steering Control for 6 × 6 Wheel-drive Mobile Robot

Hongqiang Zhao[1],Chao Luo[1],Yongkang Xu[1],Jiehao[2] Li
[1]State Key Laboratory of High Performance Complex Manufacturing,
School of Mechanical and Electrical Engineering,Central South University
ChangSha, China
[2]State Key Laboratory of Intelligent Control and Decision of Complex Systems
School of Automation, Beijing Institute of Technology
Beijing, China
*E-mail:zhaohq9922@sina.com;193712199@csu.edu.cn;xuyongkang@csu.edu.cn;jiehao.li@ieee.org

***Abstract*—The 6 × 6 Wheel-drive mobile robot is widely used in the field of special operations, and there is the phenomenon of slipping in the process of steering. To study the steering accuracy and stability of mobile robot, the dynamic model of 6 × 6 Wheel-drive Mobile Robot is established, and the sliding mode control strategy of differential steering based on mobile robot is proposed. Firstly, taking the torque of six wheels and the operator's direction control as input, the three-dimensional attitude and the relative position of the steering center of the mobile robot are obtained by using the position and attitude sensor, to determine the reference steering angle of the mobile robot. Secondly, considering the relationship between the position error and the velocity error, a recursive sliding surface is designed, and a neural network is introduced to approach the uncertain part of the mobile robot model. Then, a nonlinear gain function is applied to construct a dynamic surface control law. Finally, through the Trucksim/Simulink co-simulation model, the nonlinear gain recursive sliding mode dynamic surface adaptive control method for mobile robot trajectory tracking can improve the tracking speed and control precision, and the control force and torque are smooth and reasonable. The results show that the method is effective in improving the steering accuracy and stability of mobile robot.**

***Keywords-component*—Distributed drive; Differential steering; Steering stability; Sliding mode control**

I. INTRODUCTION

As one of the components of the unmanned system, the ground mobile robot can autonomously perform tasks such as ground transportation. This typical intelligent transportation system is widely used in the field of special operations due to its excellent safety, mobility and autonomy [1] [2].

The 6 × 6 Wheel-drive Mobile Robot studied in this paper is a long-distance line-of-sight operating platform. The platform uses 6 in-wheel motors to independently drive the wheels. After testing the platform, it was found that the remote control was used to issue a steering command, and after the controller assigned the corresponding driving torque to the 6 hub motors, the vehicle produced a lateral displacement phenomenon, which caused the mobile robot to deviate from the trajectory [3]. For such problems, many scholars have conducted research based on the driving stability control algorithm of the mobile robot.

Maclaurin B et al. took 6×6 differential steering vehicles as the research object, and compared and analyzed the steering performance of differential steering and Ackerman steering vehicles [4]. In order to improve the handling and stability of the vehicle, Kyongsu Yi et al. conducted an in-depth study of the wheel torque distribution algorithm for six-wheel speed differential steering vehicles, including modeling of factors such as wheel slip rate limitation and actuator model errors, and compared the differential steering control. The handling performance of vehicles and traditional vehicles [5]. Ge Yinghui and others mainly studied the electronic differential control of micro-electric vehicles, integrated the switch control of wheel torque distribution and wheel slip rate, and proposed the use of BP neural network PID control method to coordinate the driving torque, and concluded: torque coordination Control can enhance the dynamics of the vehicle and the extreme driving performance of the curve, and improve the handling and stability of the vehicle [6].

According to the nonlinear characteristics and model uncertainty of vehicle dynamics, Mirzaeinejad et al. designed a nonlinear controller with enhanced robustness. The continuous nonlinear vehicle dynamics model was used to predict the wheel skating response of ABS and proposed a Based on the optimized braking torque vacancy rate, a completely smooth control input that is easy to implement is obtained [7]. Jawad Aslam and others studied the dynamic feedback control method of four-wheel speed difference steering vehicles, and designed a fuzzy-sliding mode controller, which effectively eliminated the bucket vibration phenomenon of the traditional sliding mode controller and enhanced the robustness of the control system [8]. Economou J T proposed the fuzzy control logic of wheeled speed differential steering electric drive vehicle based on actual vehicle test data to simulate the interaction between the vehicle and the ground during steering [9].

In this paper, the dynamic surface adaptive control method of mobile robot trajectory tracking using nonlinear gain recursive sliding mode is presented, and the mobile robot is verified and tested based on the combined simulation of Trucksim and Simulink.

II. MOBILE ROBOT DYNAMIC MODEL

This article uses the six-wheel mobile robot model shown in Figure 1. The distances from the center of the vehicle body to the front and rear wheels are l_f and l_r, respectively, where $l_f = l_r = l/2$. There is no distance between the center of the car body and the middle wheel.

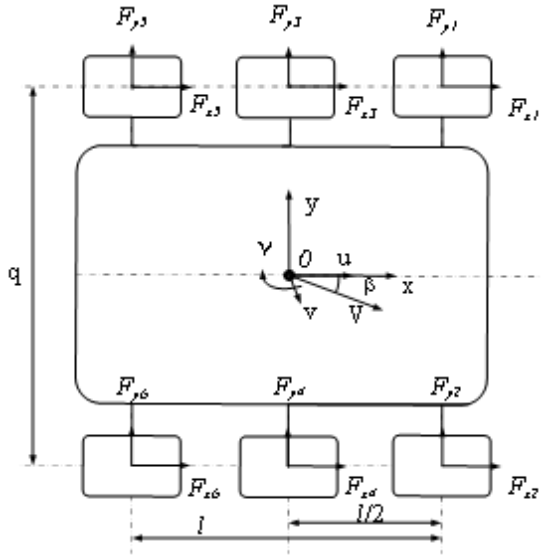

Figure 1. Wheel-drive Mobile Robot

The following equation of motion represents the dynamic equation of the high-speed motion of the six-wheel mobile robot.

$$mV_x(\dot{\beta} + \gamma) = \sum_{i=1}^{6} F_{yi} \tag{1}$$

$$\begin{aligned} I_z\dot{\gamma} = &\left[\frac{b}{2}(F_{x2} + F_{x4} + F_{x6} - F_{x1} - F_{x3} - F_{x5})\right] \\ &+ \left[\frac{l}{2}(F_{y1} + F_{y2}) - \frac{l}{2}(F_{y5} + F_{y6})\right] \end{aligned} \tag{2}$$

$$M_z = \frac{d}{2}(F_{x2} + F_{x4} + F_{x6} - F_{x1} - F_{x3} - F_{x5}) \tag{3}$$

$$M_d = \frac{l}{2}(F_{y1} + F_{y2}) - \frac{l}{2}(F_{y5} + F_{y6}) \tag{4}$$

Where m is the mass of the mobile robot V_x is the longitudinal speed of the mobile robot β is the sliding angle, and the moment of inertia γ is the yaw rate d is the distance between the left and right wheels, and F_{xi} is the longitudinal force of the tire. The direct yaw moment M_z produced by the longitudinal driving force difference between the tires The steering moment M_d produced as the resistance component of the tires during turning, together form the yaw moment.

The steady-state steering angle when driving on a road with a turning radius of R is:

$$\delta = \frac{l}{R} + K_v a_y \tag{5}$$

Where K_V is the under-steer gradient, and the formula is as follows:

$$K_v = \frac{m}{4C_{\alpha f}} - \frac{m}{4C_{\alpha r}} \tag{6}$$

$$\frac{1}{R} = \frac{\delta}{l + \frac{mV_x^2(lC_{\alpha r} - lC_{\alpha f})}{4lC_{\alpha r}C_{\alpha f}}} \tag{7}$$

The vertical force of the tire changes with the longitudinal acceleration a_y and the lateral acceleration a_x, as shown in (8).

$$\begin{aligned} F_{z1} &= \frac{mg}{6} - \frac{m_s a_x h_s}{2l} - k_f \frac{m_s a_y h_s}{d} \\ F_{z2} &= \frac{mg}{6} - \frac{m_s a_x h_s}{2l} + k_f \frac{m_s a_y h_s}{d} \\ F_{z3} &= \frac{mg}{6} - k_m \frac{m_s a_y h_s}{d} \\ F_{z4} &= \frac{mg}{6} + k_m \frac{m_s a_y h_s}{d} \\ F_{z5} &= \frac{mg}{6} + \frac{m_s a_x h_s}{2l} - k_r \frac{m_s a_y h_s}{d} \\ F_{z6} &= \frac{mg}{6} + \frac{m_s a_x h_s}{2l} + k_r \frac{m_s a_y h_s}{d} \end{aligned} \tag{8}$$

Where m is the sprung mass, h_s is the sprung mass height.g is the gravitational constant k_f and k_r are the lateral weight offset distributions of the front and rear wheels, respectively.

The absolute speed of mobile robots $\begin{bmatrix}\dot{x} & \dot{y} & \dot{\theta}\end{bmatrix}^T$ converted in the local coordinate system to $\begin{bmatrix}\dot{u} & \dot{v} & \dot{r}\end{bmatrix}^T$:

$$\begin{bmatrix}\dot{x} \\ \dot{y} \\ \dot{\theta}\end{bmatrix} = \begin{bmatrix}cos\theta & -sin\theta & 0 \\ sin\theta & cos\theta & 0 \\ 0 & 0 & 1\end{bmatrix} \begin{bmatrix}u \\ v \\ r\end{bmatrix} \tag{9}$$

Among them, u represents the x-axis velocity component of the unmanned platform in the local coordinate system, v represents the y-axis velocity component, and r represents the angular velocity.

Analyze and calculate the rotational movement of the six wheels of the mobile robot, and obtain the equation of motion as:

$$\begin{cases} J_i\dot{\omega}_i = T_{ei} - F_{xi}R - T_{fi} \\ T_{fi} = F_{fi}R \end{cases} \tag{10}$$

III. 6×6 MOBILE ROBOT TRUCKSIM MODEL

This article chooses TruckSim software to build a multi-wheel mobile platform. In this software, the power transmission system is removed from the model, Simulink co-simulation is used to import the in-wheel motor structure, and the torque signal of the control algorithm is directly applied to the tire.

The development data of Trucksim mobile robot model includes sprung mass, inertia and size parameters; K&c data of suspension system.

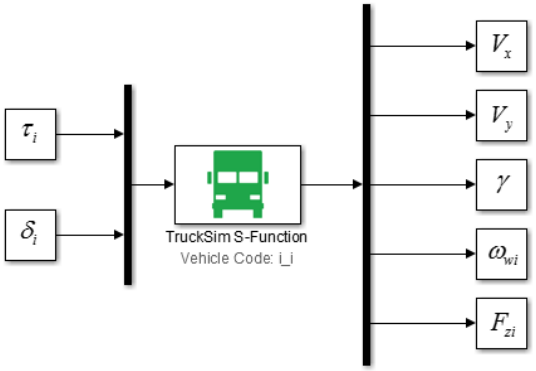

Figure 2. The input and output of the Trucksim model

Figure 2 and Table 1 show the input and output of the TruckSim model. The driving force generated by the six torque values is applied to the mobile robot model. Output includes longitudinal/lateral speed, yaw rate, wheel speed and vertical force.

TABLE I
TRUCKSIM VEHICLE MODEL INPUTS AND OUTPUTS

symbol	definition
τ_i	Torque of each wheel drive wheel(i=1-6)
δ_i	Direction input
V_x	Longitudinal speed
V_y	Lateral speed
γ	Yaw rate
ω_{wi}	Speed of each wheel
F_{zi}	Vertical force of each wheel(i=1-6)

Trucksim software can handle the non-linearity related to tire longitudinal and lateral movement and wheel and camber angle changes, and use control algorithms to calculate the steering angle of each wheel. The power structure of the 6 × 6 Wheel-drive Mobile Robot is shown in Figure 3.

Through the analysis of the main structure and parameters of the 6 × 6 Wheel-drive Mobile Robot, the main parameters for the Trucksim model of the mobile robot are shown in Table 2.

TABLE II
SIMULATION PARAMETERS OF MOBILE ROBOT MODEL

Parameters/units	Numerical value
$Length \times width \times height/mm$	4285 × 1950 × 1500
Vehicle quality/Kg	2100
Wheelbase/mm	1600
Distance from center of mass to front axle/mm	1600
Center of mass height/mm	800

With reference to the tire modeling parameters in Trucksim, the relationship curve between wheel slip and longitudinal adhesion coefficient can be drawn, as shown in Figure 4. Within a certain range, the tire longitudinal adhesion coefficient and the tire slip rate show a proportional trend; beyond the range, the tire's longitudinal adhesion coefficient and the tire slip

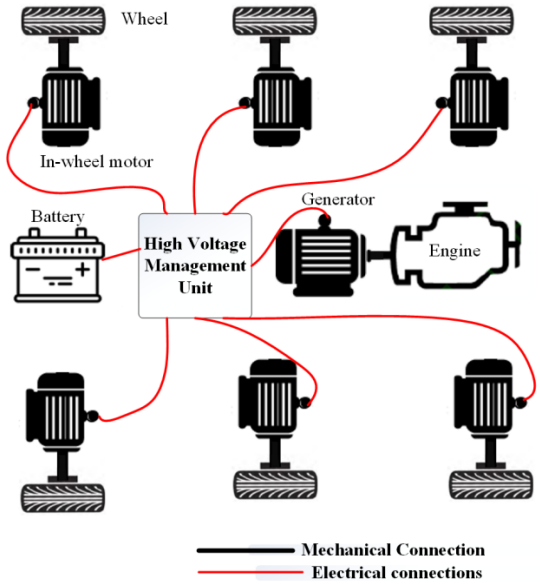

Figure 3. Schematic diagram of six-wheel drive mobile robot

rate show an inverse relationship. In summary, it can be seen that the lateral adhesion coefficient of mobile robot wheels decreases rapidly with the increase of slip rate.

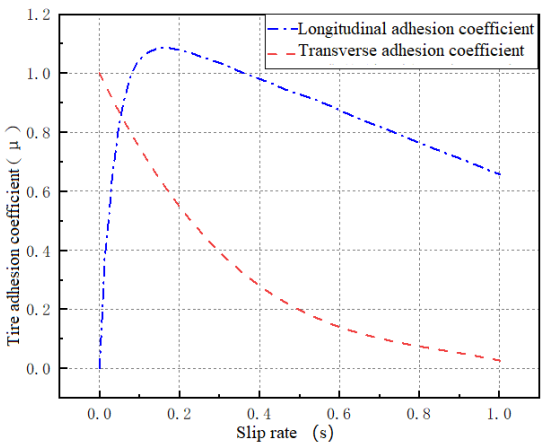

Figure 4. The relationship between tire adhesion coefficient and slip rate

IV. CONTROL SYSTEM DESIGN

Considering the uncertain part of the trajectory tracking ship model and the disturbance of the external environment, a new simple nonlinear gain function and recursive sliding surface are introduced. Combined with neural network, dynamic surface technology and adaptive robust inversion technology, an adaptive neural network controller with nonlinear gain recursive sliding mode is designed for the trajectory tracking dynamic surface of mobile robot.

In order to solve the contradiction between the control accuracy and dynamic quality of the conventional dynamic surface control system based on linear gain setting, a nonlinear gain function is designed:$s_1 \in R^3$.

$$g(x) = a|x|^{0.5} sgn(x) \tag{11}$$

Among them, $a > 0$. This function has the excellent properties of "small error, large gain, large error, small gain",that is, a slightly smaller gain is used when the error is large, and the gain is increased when the error is small. In this way, the error will not be too small and the coefficient will not be large, resulting in slow approach to the target value.The function can effectively solve the above contradiction. In the conventional dynamic surface method, the introduction of nonlinear gain function increases the difficulty of proving the stability of Lyapunov function, which will be solved by using recursive sliding mode.

Considering the position error vector of mobile robot, the first sliding mode vector defined as

$$\begin{cases} z_1 = J^T(\varphi)(\eta - \eta_d) \\ s_1 = z_1 \end{cases} \tag{12}$$

where,$\eta_d = [x_d, y_d, \varphi_d]^T$ $a > 0$.The derivation of the above formula with respect to time can be obtained:

$$\dot{s_1} = \dot{J^T}(\varphi)(\eta - \eta_d) + J^T(\varphi)(\eta - \eta_d) \tag{13}$$

Design virtual control vector based on:

$$\alpha_1 = -K_1 l_1(s_1) + J^T(\varphi)\dot{\eta_d} - R^T(r)s_1 \tag{14}$$

According to the ship speed error vector $z_2 = v - v_d$ and the position error vector S_1, which are obtained, $s_2 \in R^3$ are considered comprehensively:

$$s_2 = C_1 s_1 + z_2 \tag{15}$$

Considering the uncertainty of parameters in the model of the 9-DOF full drive trajectory tracking mobile robot Δ_f, so three RBF neural networks $[11-13]$ are introduced to approximate it:

$$\Delta_f = W^{*T} h(z) + e(z) \tag{16}$$

In the above formula,$z = [u, v, r]^T$ is the input vector of RBF neural network; RBF neural network approximation error vector is:

$$e(z) = [e_1(z), e_2(z), e_3(z)]^T \tag{17}$$

The matrix of ideal weight vector is defined as:

$$W^* = \begin{bmatrix} \omega_1^{*T} & 0_{1\times l} & 0_{1\times l} \\ 0_{1\times l} & \omega_2^{*T} & 0_{1\times l} \\ 0_{1\times l} & 0_{1\times l} & \omega_3^{*T} \end{bmatrix}^T \tag{18}$$

Where $\omega_i^* = \left[\omega_{i,1}^*, \cdots, \omega_{i,l}^*\right]^T$, The vector composed of radial basis function is defined as $h_i(z) = [h_{i,1}(z), \cdots, h_{i,l}(z)]^T$. The Gauss basis function is usually used to construct the structure, and its expression is defined as:

$$h_{i,j} = exp\left[-\frac{(z-c_j)^T(z-c_j)}{2b_{i,j}^2}\right] \tag{19}$$

Where $j = 1 \cdots l$, $c_j = [c_{j,1}, c_{j,2}, c_{j,3}]^T$ is the vector value of the center point of the jth hidden layer neuron, $b_{i,j} > 0$ is the width of gausky function of the hidden layer neuron j of the ith neural network.

For each component of the approximation error $e(z)$ of the external disturbance d and RBF neural network of the trajectory tracking ship, there are bounded functions $\delta > 0$,make $|e_i(z)| + |d_i| < \delta_i$,the bound vectors of the approximation error $e(z)$ and the external disturbance d of the neural network can be expressed as $\delta = [\delta_1, \delta_2, \delta_3]^T$.The trajectory tracking state feedback control law of mobile robot is designed as:

$$\begin{aligned} \tau =& C(v)v + Dv + M\dot{v}_d - MC_1\dot{s}_1 + \hat{W}^T h(z) - \\ & K_2 l_2(s_2) - C_2 s_2 - N_2(s_2) l_1(s_1) - \Xi\hat{\delta} \end{aligned} \tag{20}$$

Among them $l_2(s_2) = [l(s_{2,1}), l(s_{2,2}), l(s_{2,3})]^T$,$K_2, C_2 \in R^{3\times 3}$is a diagonal matrix with positive definite parameters, $N_2(s_2) = diag\left[n_2^{-1}(s_{2,1}), n_2^{-1}(s_{2,2}), n_2^{-1}(s_{2,3})\right]$,$\Xi = diag\left[tanh\left(\frac{l_2(s_{2,1})}{\varepsilon_1}\right), tanh\left(\frac{l_2(s_{2,2})}{\varepsilon_2}\right), tanh\left(\frac{l_2(s_{2,3})}{\varepsilon_3}\right)\right]$,$\hat{\omega} = \begin{bmatrix} \hat{\omega}_1^T & 0_{1\times l} & 0_{1\times l} \\ 0_{1\times l} & \hat{\omega}_2^T & 0_{1\times l} \\ 0_{1\times l} & 0_{1\times l} & \hat{\omega}_3^T \end{bmatrix}^T$ is the matrix w composed of ideal weight vector W^* an estimate of the cost of the project, an estimate vector with $\hat{\delta}$ as δ.The weight vector adaptive law is designed as:

$$\dot{\hat{\omega}} = \Gamma\left[-h_i(z) l_2(s_{2,i}) - \sigma_i \hat{\omega}_i\right] \tag{21}$$

Where, $\Gamma \in R^{l\times l}$is a positive definite parameter diagonal matrix and $\sigma_i$is a positive design constant.

For the bound vectorσ, which is composed of the approximation error of neural network and the disturbance of the external environment, the adaptive law of the estimated value is designed as:

$$\dot{\hat{\sigma}} = \varrho_i\left[\Xi l_2(s_{2,i}) - \Lambda(\hat{\delta} - \delta^0)\right] \tag{22}$$

V. Simulation analysis

In this paper, Trucksim and Simulink are used for joint simulation. The car body, tires, and suspension are parametrically modeled. Simulink is used to build the in-wheel motor model, and the Simulink module is imported through the trucksim interface.

In order to reasonably analyze the steering motion model of the mobile robot, the following assumptions are made:driving on a good level road, the contact between the wheel and the ground is regarded as point contact, the center of mass is located on the longitudinal symmetry centerline of the vehicle, the road adhesion coefficient of the wheels on both sides is set to 0.1, and the initial vehicle speed of the given mobile robot is 70 km/h. With reference to the actual situation, this article limits the peak value of the motor torque to $1000Nm$.

The simulation results are shown in the figure:

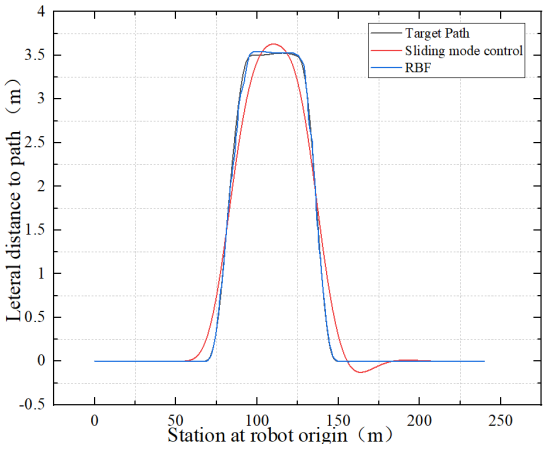

Figure 5. Trajectory map of mobile robot and target trajectory map

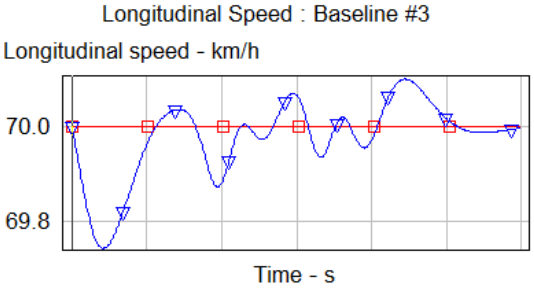

Figure 6. Mobile robot speed chart

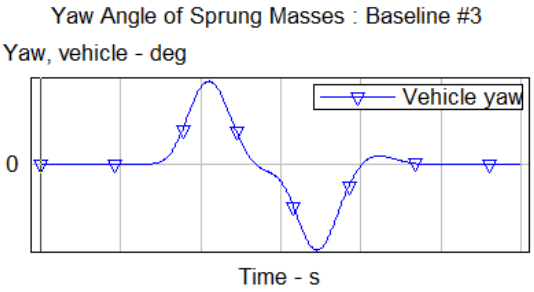

Figure 7. Yaw Angle of mobile robot

The simulation results are shown in Figure 7 to Figure 11. The results show that the yaw rate of the mobile robot is 3 (deg/s), the lateral offset is 0.35 meters, and the slip of the six wheels is small. Therefore, the mobile robot has good stability during the turning process. Analyzing the results, it can be confirmed that using the 6 × 6 Wheel-drive mobile robot with sliding model control as the carrier, the output of the six-wheel torque can be quickly equalized and maintained, the speed of the mobile robot can quickly reach the set speed, and the driving trajectory of the unmanned platform is more consistent with the target trajectory.

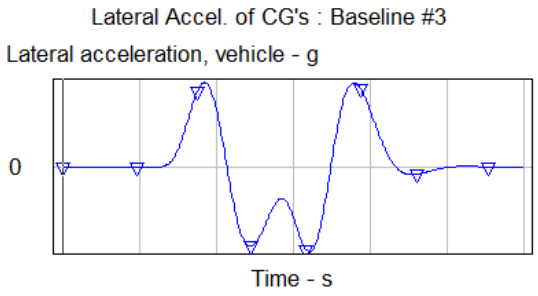

Figure 8. Transverse acceleration of mobile robot

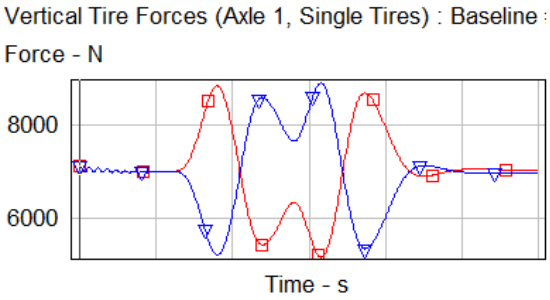

Figure 9. Force on front wheel of mobile robot

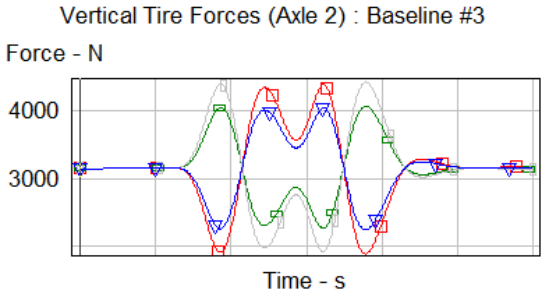

Figure 10. Force on rear wheel of mobile robot

VI. Simulation Analysis

After establishing the dynamic model of the mobile robot, use Simulink to create the wheel hub motor drive model, and combine it with the Trucksim mobile robot for parametric modeling. In this way, the advantages of the respective platforms and joint simulation can be used to make the Simulink control block without The human platform provides a stable driving force.

The Trucksim/Simulink co-simulation model of the 6 × 6 Wheel-drive Mobile Robot established in this paper can accurately reproduce the real motion state and trajectory during the steering process of the mobile robot, and predict, prevent and control deviation and roll trends. It provides a solid theoretical foundation and practical platform for the design of a steering stability control system.

The nonlinear gain recursive sliding mode dynamic surface adaptive control method for mobile robot trajectory tracking

can improve the tracking speed and control precision, and the control force and torque are smooth and reasonable. It is more suitable for the actual operation of mobile robot and has reference value in engineering practice.

REFERENCES

[1] Gage D W. History of UGV:A Brief History of Unmanned Ground Vehicle (UGV) Development Efforts[J]. Unmanned Systems Magazine,1995,13:1-9.

[2] CHEN Huiyan, ZHANG Yu. An Overview of Research on Military Unmanned Ground Vehicles[J] Journal of China Ordnance. 2014,35(10):1696-1706.

[3] Wongun Kim, Kyongsu Yi and Jongseok Lee. Development of a Driving Control Algorithm and Performance Verification Using Real-Time Simulator for a 6WD/6WS Vehicle[J]. SAE International, 2011,1(262):16-24.

[4] Maclaurin B. Comparing the steering performances of skid-and Ackermann-steered vehicles [J]. Proceedings of the Institution of Mechanical Engineers, 2008, 222(5):739-756.

[5] Nah J, Yi K, Kim W, et al. Torque distribution algorithm of six-wheeled skid-steered vehicles for on-road and off-road maneuverability[R].SAE Technical Paper,2013, 15(5): 64-78.

[6] Mirzaeinejad H, Mirzaei M. A novel method for non-linear control of wheel slip in anti lock braking systems[J]. Control Engineering Practice, 2010, 18(8): 918 926.

[7] Jawad Aslam, Shi-Yin Qin, Muhammad Adnan Alvi. Fuzzy sliding mode control algorithm for a four-wheel skid steer vehicle[J]. Journal of Mechanical Science and Technology, 2014,28(8):3301-3310.

[8] Economou J T, Colyer R E. Modelling of skid steering and fuzzy logic vehicle ground interaction[C]. American Control Conference 2000. IEEE, 2000, 1(6): 100-104.

[9] Guangcai ZOU, Yugong LUO, Keqiang LI, Xiaoming LIAN. Improvement Maneuverability and stability of independent 4WD EV by DYC based on control target dynamic regulation[J]. Journal of Mechanical Systems for Transportatoin and Logistics,2008,3(1):305-318.

[10] Nam K, Fujimoto H, Hori Y. Lateral Stability Control of In-Wheel-Motor-Driven Electric Vehicles Based on Sideslip Angle Estimation Using Lateral Tire Force Sensors[J]. IEEE Transactions on Vehicular Technology, 2012, 61(5):1972-1985.

[11] Li, J., Wang, J., Peng, H., Hu, Y., and Su, H. (2021), "Fuzzy-torque approximation enhanced sliding mode control for lateral stability of mobile robot", IEEE Transactions on Systems, Man, and Cybernetics: Systems, doi: 10.1109/TSMC.2021.3050616.

[12] Li, J., Qin, H., Wang, J., and Li, J.(2021), "Open Street Map-based autonomous navigation for the four wheel-legged robot via 3D-Lidar and CCD camera", IEEE Transactions on Industrial Electronics, pp. 1-10, doi: 10.1109/TIE.2021.3070508.

[13] Li, J., Wang, J., Peng, H., Zhang, L., Hu, Y., and Su, H. (2020),"Neural fuzzy approximation enhanced autonomous tracking control of the wheel-legged robot under uncertain physical interaction", Neurocomputing, Vol. 410, pp. 342-353.

[14] Li, J., Wang, J., Wang, S., Peng, H., Wang, B., Qi, W., Zhang, L., and Su, H. (2020),"Parallel structure of six wheel-legged robot trajectory tracking control with heavy payload under uncertain physical interaction", Assembly Automation. Vol. 40 No. 5, pp. 675-687.

[15] Huang, D., Yang, C., Pan, Y., & Cheng, L. (2019). Composite learning enhanced neural control for robot manipulator with output error constraints.IEEE Transactions on Industrial Informatics,17(1), 209-218.

[16] Yang, C., Zeng, C., Cong, Y., Wang, N., & Wang, M. (2018). A learning framework of adaptive manipulative skills from human to robot.IEEE Transactions on Industrial Informatics,15(2), 1153-1161.

[17] Yang, C., Huang, D., He, W., & Cheng, L. (2020). Neural control of robot manipulators with trajectory tracking constraints and input saturation.IEEE Transactions on Neural Networks and Learning Systems., 1-12, doi: 10.1109/TNNLS.2020.3017202.

[18] Chen Z, Wang S, Wang J, et al. Control strategy of stable walking for a hexapod wheel-legged robot[J]. ISA transactions, 2021, 108: 367-380.

[19] Chen Z, Wang S, Wang J, et al. Attitude stability Control for Multi-Agent Six Wheel-Legged Robot[J]. IFAC-PapersOnLine, 2020, 53(2): 9636-9641.

[20] Chen Z, Li J, Wang J, et al. Towards Hybrid Gait Obstacle Avoidance for a Six Wheel-Legged Robot with Payload Transportation[J]. Journal of Intelligent & Robotic Systems, 2021, 102(3): 1-21.